Journal of Materials Chemistry

Cite this: J. Mater. Chem., 2012, 22, 2299

www.rsc.org/materials

PAPER

Regulating mesogenic properties of ionic liquid crystals by preparing binary or multi-component systems†

Meng Wang, Xu Pan, Shangfeng Xiao, Changneng Zhang, Wenxin Li and Songyuan Dai*

Received 26th September 2011, Accepted 3rd November 2011
DOI: 10.1039/c1jm14790k

In this study, a series of binary systems based ionic liquid crystals (ILCs) $C_{12}MIm(BF_4)_yI_x$ ($x + y = 1$) are prepared by mixing ILCs 1-dodecyl-3-methylimidazolium iodide ($C_{12}MImI$) and 1-dodecyl-3-methylimidazolium tetrafluoroborate ($C_{12}MImBF_4$), aiming to combine the properties of both $C_{12}MImBF_4$ and $C_{12}MImI$. Their mesogenic properties are characterized by thermal analysis, polarized optical microscopy, X-ray diffraction as well as anisotropic ionic conductivity measurements. It is found that the smectic A phase with interdigitated bilayer structure is observed in the $C_{12}MIm(BF_4)_yI_x$ series. The binary system $C_{12}MIm(BF_4)_yI_x$ has a larger mesophase temperature range and interdigitated layer spacing than pure $C_{12}MImBF_4$. And the anisotropic ionic conductivity of the binary system, including parallel and perpendicular to smectic layer, is higher than pure $C_{12}MImI$. Moreover, in binary system $C_{12}MIm(BF_4)_yI_x$, with the increasing content of $C_{12}MImI$ the ability of the anion to form three dimensional hydrogen bonds increases, resulting in the increase of the mesophase temperature range, interdigitated layer spacing and the decrease of anisotropic ionic conductivity. Furthermore, multi-component system based ILCs are obtained by introducing iodine to the binary system, and the mesophase temperature range is lowered, which is associated with the weak ability of I_3^- to form hydrogen bond with cations. All these results suggest that we can regulate the mesogenic properties of ILCs as we need by making binary or even multi-component systems.

1. Introduction

Ionic liquids (ILs) are molten salts with melting points at or below ambient temperature, which have attracted great interest due to their unique properties, including nonvolatility, nonflammability, good thermal stability, and high ionic conductivity.[1–3] Liquid crystals (LCs) are considered as the "fourth state of matter", whose properties are intermediate between that of the crystalline solid state and that of the liquid state. The merger of ILs and LCs has yielded a new class of materials called ionic liquid crystals (ILCs). ILCs can be considered as substances that combine the properties of both ILs and LCs. Some properties of ILCs differ significantly from not only those of conventional neutral organic LCs, but also conventional ionic liquids because of their anisotropic character caused by the self-organized orientational ordering at the nanometre level.[4] For instance, ionic conductivity was enhanced in the smectic A and columnar phases compared to that in the isotropic phase.[5] Thus, they have exhibited interesting potential applications as ion conductive materials in electrochemical devices,[6] as organized reaction media for the selectivity for organic reactions,[7,8] and as templating agents for functional nanostructured materials in materials science.[9]

Because of the widespread application of imidazolium-based ILs, imidazolium-based ILCs have been frequently studied.[10–12] Many studies are focused on the 1-alkyl-3-methylimidazolium salts based ILCs. The smectic phase with lamellar structure is commonly obtained for imidazolium-based ILCs. Generally, with the increase of the long alkyl chain attached to the N^1-position of the imidazolium ring, the mesophase temperature range increases drastically, while the anisotropic ionic conductivity decreases.[13] Additionally, some groups have also studied counterion effects on mesogenic properties. Examples of liquid crystalline 1-alkyl-3-methylimidazolium salts containing different anions such as chloride,[14] bromide,[15] hexafluorophosphate[10] and tetrafluoroborate[11] have been reported, which shows that the counterion has a great effect on the mesogenic properties of ILCs. All these efforts have been made to explore a kind of ILCs with a large mesophase temperature range and a high anisotropic ionic conductivity for further application. However, a phenomenon is usually observed that one material has a relatively larger mesophase temperature range but lower anisotropic ionic conductivity, while another material has larger anisotropic ionic conductivity

Key Laboratory of Novel Thin Film Solar Cells, Institute of Plasma Physics, Chinese Academy of Sciences, P. O. Box 1126, Hefei, Anhui, 230031, P. R. China. E-mail: sydai@ipp.ac.cn; Fax: +86-551-5591377; Tel: +86-551-5591377

† Electronic supplementary information (ESI) available: details about ^{1}H-NMR data, DSC traces of $C_{12}MIm(BF_4)_yI_x$, POM textures, interdigitated bilayer structure of $C_{12}MIm(BF_4)_{0.4}I_{0.45}(I_3)_{0.15}$, measurements of anisotropic ionic conductivity. See DOI: 10.1039/c1jm14790k

but a lower mesophase temperature range. For example, imidazolium salts with fluorinated anions tend to have higher anisotropic ionic conductivity than compounds with nonfluorinated anions,[13,16] but a lower mesophase temperature range.[17] Thus, this triggered our interest to explore a new type of ILCs to combine the advantages of two different ILCs.

Herein, a series of binary systems based ILCs were successfully prepared by mixing ILCs 1-dodecyl-3-methylimidazolium iodide (C_{12}MImI) and 1-dodecyl-3-methylimidazolium tetrafluoroborate (C_{12}MImBF_4), aiming to combine the advantages of both C_{12}MImI and C_{12}MImBF_4. The reason why ILCs with the same cations are chosen is that the imidazolium cation plays the most important role on the mesogenic properties. Besides, incorporation of C_{12}MImBF_4 into the binary systems based ionic liquid crystals $C_{12}MIm(BF_4)_yI_x$ ($x + y = 1$) may lead to high anisotropic ionic conductivity, since fluoroborate ionic liquids exhibit high conductivity.[18] The mesogenic properties of binary systems $C_{12}MIm(BF_4)_yI_x$ were characterized by several techniques, including differential scanning calorimetry (DSC), polarized optical microscopy (POM), and small-angle X-ray diffraction (SAXD). The anisotropic ionic conductivity of $C_{12}MIm(BF_4)_yI_x$ was also measured for the liquid crystalline mesophase. Furthermore, multi-component system based ILCs were prepared by introducing iodine to the binary system. The mesogenic properties of a multi-component system as well as diffusion of I_3^- in the multi-component system were also studied.

2. Experimental section

2.1 Materials

All reagents are purchased from Acros and used as received.

2.2 Synthesis

Synthesis of 1-dodecyl-3-methylimidazolium iodide (C_{12}MImI). C_{12}MImI was synthesized by the quaternization of 1-methylimidazole and 1-iododecane. The mixture of 1-methylimidazole and 1-iododododecane was dissolved in acetone. Then the solution was placed into a 58 mL Teflon lined, stainless steel autoclave and heated at 100 °C for 12 h. The crude product was washed with diethyl ether several times and the pale yellow viscous liquid C_{12}MImI was obtained with a yield of 90.5%. The purity of C_{12}MImI was identified by ^{1}H-NMR (see ESI†).

Synthesis of 1-dodecyl-3-methylimidazolium tetrafluoroborate (C_{12}MImBF_4). A solution of 1-dodecyl-3-methylimidazolium iodide (C_{12}MImI) (3.378 g, 10 mmol) in acetone (50 mL) was added slowly to a rapidly stirred solution of $AgBF_4$ (2.04 g, 10.5 mol) in acetone (20 mL) and stirring continued until no residual C_{12}MImI was detected with the use of $AgNO_3$ in acetone. The solvent of the filtrate was removed by rotary evaporation, then the crude product was dissolved in dichloromethane (50 mL) and washed with water (3 × 40 mL). The organic layer was collected, dried over $MgSO_4$, filtered and the solvent was removed *in vacuo* to yield the C_{12}MImBF_4 colourless liquid with a yield of 88.5%. The purity of C_{12}MImBF_4 was identified by ^{1}H-NMR as well (see ESI†).

Preparations of binary and multi-component systems. To make the mixture of C_{12}MImI and C_{12}MImBF_4 homogeneous, different molar ratios of C_{12}MImI and C_{12}MImBF_4 were dissolved in vigorously stirred solvent (acetone). Then the solvent was removed *in vacuo* to yield the binary system based ILCs. The multi-component system was prepared by introducing iodine to a certain binary system followed by heating and re-cooling, then repeated at least three times, by which stage it was assumed that a homogeneous multi-component system had been made.

2.3 Analytical measurements

Differential scanning calorimetry (DSC) was performed with a computer controlled thermal analyzer (DSC Q2000, TA Instruments, America) with nitrogen as protection gas. The samples were placed in aluminium pans which were cold-sealed under nitrogen. Experimental data are displayed in such a way that exothermic peaks occur at positive heat flow and endothermic peaks at negative heat flow. Heating and cooling rates were set as 10 K min^{-1}.

Polarized optical microscopy (POM) was performed using an Olympus BX-51 microscope (Japan) equipped with a hot stage under cross-polarized light at 100× magnification. The samples were placed between two cover slips and inserted into the hot stage. The temperatures of all samples were fixed at 35 °C.

The small angle X-ray powder diffraction patterns of imidazolium salts were determined using a TTRAX3 diffractometer with Cu-Kα X-rays, $\lambda = 1.542$ Å (Rigaku, Japan). Data were recorded from between 1 and 10° in steps of 0.02° at 300 K.

The anisotropic ionic conductivity was measured by the impedance technique using an Im6e workstation (Zahner-Elektrick, German). Ionic conductivities, including parallel ($\sigma_{\parallel}$) and perpendicular to smectic layers ($\sigma_{\perp}$), were measured according to the previously reported method.[5,13,19,20] A pair of Cu electrodes was used to measure $\sigma_{\parallel}$ (Fig. S2† and S3†). A Cu electrode (about 150 μm in thickness) was placed on a glass substrate. The sample was placed in the region between two Cu electrodes and covered with a piece of glass substrate to help the formation of the alignment. A pair of FTO (F-doped tin oxide) glass electrodes was used to measure $\sigma_{\perp}$,[21] (Fig. S4† and S5†). The sample was sandwiched with two FTO glass electrodes and fixed with a Teflon spacer (300 μm in thickness). The cell constants of these cells were calibrated with a standard KCl aqueous solution at room temperature and the change of cell constant with increasing temperature is neglected.

The steady-state voltammetry of the multi-component system was adopted in a conventional electrochemical cell equipped with a 10 μm platinum ultra-microelectrode (CHI107) as working electrode, and with a 1 mm radius platinum disk electrode (CHI102) as counter electrode and reference electrode. A slow scan rate (5 mV s^{-1}) was used in order to obtain steady-state current–voltage curves. This work was carried out at 300 K on an electrochemical workstation (CHI660A, CH Instruments Inc., Austin, TX).

3. Results and discussion

3.1 Binary systems

3.1.1 Thermal behavior of $C_{12}MIm(BF_4)_yI_x$. From the DSC traces (Fig. S1†), it can be seen that a mesophase is observed for C_{12}MImI, C_{12}MImBF_4 and binary systems $C_{12}MIm(BF_4)_yI_x$

($x + y = 1$). The DSC data obtained from the DSC curves (phase transition temperatures and phase transition enthalpies, ΔH) are listed in Table 1 and Fig. 1. Obviously, $C_{12}MImI$ has a relatively larger mesophase temperature range than $C_{12}MImBF_4$. With the increasing x from 0.2 to 0.8, the clearing point of $C_{12}MIm(BF_4)_yI_x$ increases significantly (except $C_{12}MIm(BF_4)_{0.8}I_{0.2}$), while the melting point varies little. As a result, the mesophase temperature range increases with increasing x in $C_{12}MIm(BF_4)_yI_x$, which suggests that the mesophase temperature range can be regulated by making a binary system.

As reported, hydrogen bonding between anions and protons of imidazolium cations plays an important part in the formation and the stability of a mesophase.[16,22] The anion BF_4^- is a coordination ion and composed of the central atom (B) and co-ordinate ions (F). Herein, the hydrogen bonds between anions and protons of imidazolium cations in tetrafluoroborate salts are formed between F and protons. Charge density (ρ) is used to characterize the hydrogen bond acceptor abilities of halides in this type of anions, and ρ can be calculated by the following equation,[10,23]

$$\rho = \frac{z^2}{n} \quad (1)$$

Where, z is the overall charge on the ion and n is the number of halide atoms in the complex. When $\rho < 1$, it will drastically weaken the hydrogen bond between halide and cations. For BF_4^-, the charge density of F is <1. As a result, compared with iodide, the ability of the anions to form a three dimensional hydrogen bond will obey the following relationship,

$$BF_4^- < I^- \quad (2)$$

Generally, the hydrogen bond between anions and protons of imidazolium cations exerts a positive effect on the formation of a mesophase. Therefore, it is easily understood that the mesophase temperature range of pure $C_{12}MImI$ is larger than that of pure $C_{12}MIm\ BF_4$. As for binary system $C_{12}MIm(BF_4)_yI_x$, the ability of the anions to form a three dimensional hydrogen bond will obey the following relationship,

$$BF_4^- < (BF_4)_yI_x < I^- \quad (3)$$

Thus, the mesophase temperature ranges of binary system $C_{12}MIm(BF_4)_yI_x$ are intermediate between pure $C_{12}MImBF_4$ and $C_{12}MImI$. Combining eqns (1), (2) and (3), we can see that with the increase of x, the ability of $[(BF_4)_yI_x]^-$ to form three dimensional hydrogen bonds with imidazolium cations increases, resulting in the increase of the mesophase temperature range of $C_{12}MIm(BF_4)_yI_x$. Thus, it is suggested that the mesophase

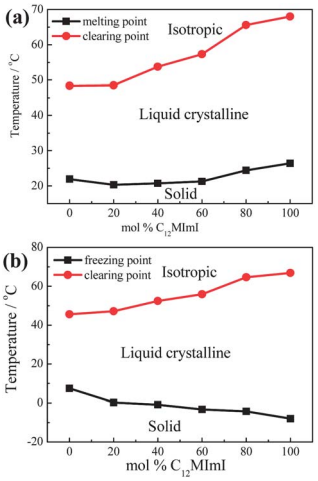

Fig. 1 The phase transition of $C_{12}MIm(BF_4)_yI_x$ in (a) the heating process and (b) the cooling process.

Table 1 A summary of the thermal analysis for the $C_{12}MIm(BF_4)_yI_x$ series

	Heating		Cooling		
$C_{12}MIm(BF_4)_yI_x$	T/(°C)	ΔH/(kJ mol^{-1})	T/(°C)	ΔH/(kJ mol^{-1})	Phase transition
$C_{12}MImBF_4$	48.38	0.09	45.61	−0.07	[a]Lc–L
	21.93	11.99	7.47	−4.91	S–Lc
	−14.9	−3.17	2.3	−0.81	[b]S1–S
$C_{12}MIm(BF_4)_{0.8}I_{0.2}$	48.54	0.29	47.17	−0.26	Lc–L
	20.3	31.73	0.23	−15.25	S–Lc
	−12.64	−15.39	—	—	S1–S
$C_{12}MIm(BF_4)_{0.6}I_{0.4}$	53.77	0.37	52.42	−0.27	Lc–L
	20.73	2.95	−0.86	−14.51	S–Lc
	18.04	1.73	—	—	S1–S
	−5.65	−11.16	—	—	[b]S2–S1
$C_{12}MIm(BF_4)_{0.4}I_{0.6}$	57.32	0.30	55.87	−0.28	Lc–L
	21.26	2.03	−3.28	−14.51	S–Lc
	16.9	12.21	—	—	S1–S
	−12.73	−11.91	—	—	S2–S1
$C_{12}MIm(BF_4)_{0.2}I_{0.8}$	65.58	0.40	64.61	−0.32	Lc–L
	24.42	3.50	−4.27	−14.91	S–Lc
	16.85	11.05	—	—	S1–S
	−10.58	−12.86	—	—	S2–S1
$C_{12}MImI$	68.01	0.42	66.84	−0.31	Lc–L
	26.4	1.66	−8.03	−13.68	S–Lc
	18.1	12.73	—	—	S1-S
	−3.28	−10.91	—	—	S2–S1

[a] The symbols S, Lc, and L denote crytstal, liquid crystal and isotropic liquid. [b] "S2–S1" and "S1-S" denote the phase transition from solid to solid.

temperature range of $C_{12}MIm(BF_4)_yI_x$ can be regulated by altering the proportion of the composition, namely, the driving forces for the formation of the mesophase.

Additionally, it should also be noted that the melting transition for $C_{12}MIm(BF_4)_yI_x$ (x from 0.4 to 0.8) isn't a sharp transition as observed for pure $C_{12}MImBF_4$, but is spread several degrees. This phenomenon is reflected by the broad peaks for $C_{12}MIm(BF_4)_{0.4}I_{0.6}$, $C_{12}MIm(BF_4)_{0.6}I_{0.8}$ and $C_{12}MIm(BF_4)_{0.8}I_{0.2}$ (Fig. S1†), which may be associated with the existence of $C_{12}MImI$ in $C_{12}MIm(BF_4)_yI_x$. While in the cooling process, the peak is sharp at the phase transition from liquid crystalline to solid, which is different from that in heating process. Furthermore, in the cooling process, both the clearing point and freezing point of $C_{12}MIm(BF_4)_yI_x$ can also be regulated by altering the proportion of the composition, and the mesophase for $C_{12}MIm(BF_4)_yI_x$ obtained in the cooling process is larger than that observed in the heating process due to the extensive supercooling before crystallization (Fig. 1b).

3.1.2 Structural properties $C_{12}MIm(BF_4)_yI_x$. The smectic phase with lamellar structure is commonly obtained for four types of ILCs (ammonium, phosphonium, imidazolium and pyridinium salts), and there is no exception for $C_{12}MImBF_4$[11] and $C_{12}MImI$.[6,24] Since the cation dominates formation of the smectic layer[10,14,17] and $C_{12}MImI$ has the same cations as $C_{12}MImBF_4$, it can be inferred that the mesophase of binary systems $C_{12}MIm(BF_4)_yI_x$ are also smectic A phase (SmA). Fig. 2 shows the polarized optical microscopic (POM) texture of $C_{12}MIm(BF_4)_{0.4}I_{0.6}$, which is typical of the $C_{12}MIm(BF_4)_yI_x$ series. It is obvious that focal conic fan textures with dark homeotropic areas are observed. The dark homeotropic areas are caused by rod-like molecules aligned parallel to the light source. The focal conic fan textures originate from the formation of layered structure. This result of the POM suggests that the liquid crystalline mesophase of $C_{12}MIm(BF_4)_yI_x$ is assigned to the SmA mesophase and a lamellar structure which has an average direction perpendicular to the layer surface is proposed.

To study the structural properties of $C_{12}MIm(BF_4)_yI_x$ in detail, small-angle X-ray diffraction (SAXD) is performed for $C_{12}MIm(BF_4)_yI_x$ at 300 K in which the $C_{12}MIm(BF_4)_yI_x$ series, including pure $C_{12}MImI$ and $C_{12}MImBF_4$, are in SmA phase (Fig. 3). Only one peak is observed for all samples, suggesting the loss of positional ordering in the layer plane due to melting of the long alkyl chain.[13] With the increasing x, the peak shifts to the lower angle region slightly, implying that the proportion of the composition in $C_{12}MIm(BF_4)_yI_x$ would exert a slight effect on the structure of the SmA meophase. Fig. 4 shows layer spacings (d) of $C_{12}MIm(BF_4)_yI_x$ plotted against x. It is seen that d of $C_{12}MImBF_4$ is smaller than that of $C_{12}MImI$ and the layer spacing d of the $C_{12}MIm(BF_4)_yI_x$ series is intermediate that of pure $C_{12}MImI$ and pure $C_{12}MImBF_4$. With the increase of x, d values gradually increases. Besides, the layer spacing d is found to satisfy $l < d < 2l$, where l is the fully extended length of the cation and is roughly estimated from crystallographic data.[25–27] This result indicates an interdigitated bilayer structure is formed in the SmA liquid crystalline mesophase[17] for $C_{12}MIm(BF_4)_yI_x$ as shown in Fig. 5.

As the $C_{12}MIm(BF_4)_yI_x$ series has the same cation, the difference in layer spacings d is mainly associated with the anions. Bradley and co-workers[17] have systematically investigated the influence of anions on the structure of the SmA liquid crystalline mesophase by using the small-angle X-ray scattering technique. They found that the ability of anions to form a three dimensional hydrogen bond would exert a significant effect on the layer spacing d. Generally, anions forming a strong three dimensional hydrogen bond with cations will help enlarge the layer spacing d. According to eqn (3), with the increase of x, the ability of $[(BF_4)_yI_x]^-$ to form a three dimensional hydrogen bond with imidazolium cations increases, therefore, the layer spacing d of $C_{12}MIm(BF_4)_yI_x$ increases with the increasing content of $C_{12}MImI$ in the mixture. This will influence the anisotropic ionic conductivity of the $C_{12}MIm(BF_4)_yI_x$ series as described below.

3.1.3 Anisotropic ionic conductivity of $C_{12}MIm(BF_4)_yI_x$. The anisotropic ionic conductivity of $C_{12}MIm(BF_4)_yI_x$, including parallel ($\sigma_{\parallel}$) and perpendicular ($\sigma_{\perp}$) to the smectic layer, were measured. The cell using Cu and FTO glass electrode was used for this measurement. The formation of homeotropic alignment of $C_{12}MIm(BF_4)_yI_x$ in the cell was obtained by exerting pressure on the sample using a piece of glass (Fig. S6†), which has been reported previously.[13] Fig. 6 shows the temperature dependence of $\sigma_{\parallel}$ and $\sigma_{\perp}$ for $C_{12}MIm(BF_4)_yI_x$. For the $C_{12}MIm(BF_4)_yI_x$ series, $\sigma_{\parallel}$ is at least five times higher than $\sigma_{\perp}$, suggesting the high ion mobility in the ionic layer shown in Fig. 5. It is seen that the conductivity of pure $C_{12}MImBF_4$, including $\sigma_{\parallel}$ and $\sigma_{\perp}$, is higher than that of pure $C_{12}MImI$ and the anisotropic ionic conductivities of binary systems $C_{12}MIm(BF_4)_yI_x$ are intermediate between that of pure $C_{12}MImI$ and $C_{12}MImBF_4$. With the

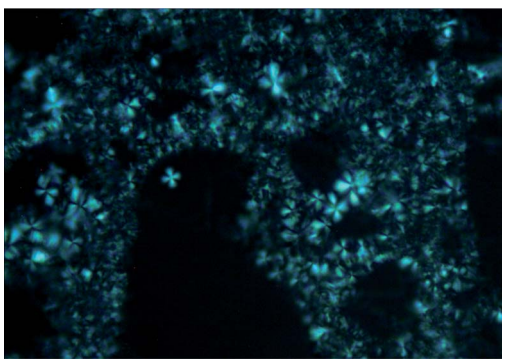

Fig. 2 The polarized optical microscopic texture of $C_{12}MIm(BF_4)_{0.4}I_{0.6}$ at 308 K.

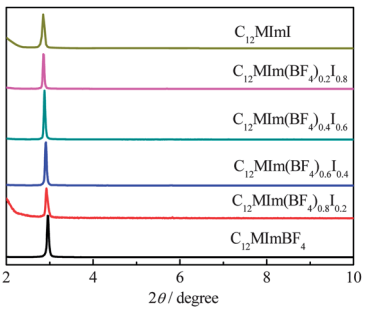

Fig. 3 SAXD patterns of the $C_{12}MIm(BF_4)_yI_x$ series at 300 K.

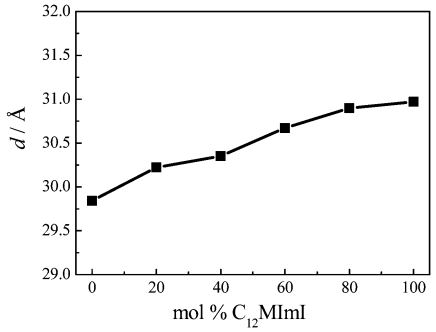

Fig. 4 Layer spacings of $C_{12}MIm(BF_4)_yI_x$ ($x = 0.2, 0.4, 0.6, 0.8$) in the liquid crystalline SmA mesophase (300 K).

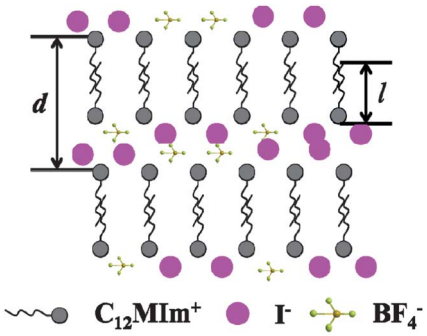

Fig. 5 A schematic illustration of the interdigitated bilayer structure of $C_{12}MIm(BF_4)_yI_x$ in the SmA liquid crystalline phase.

increase of x, both $\sigma_{\parallel}$ and $\sigma_{\perp}$ of $C_{12}MIm(BF_4)_yI_x$ decrease, indicating that the anisotropic ionic conductivity of $C_{12}MIm(BF_4)_yI_x$ can also be regulated by varying the proportion of the composition.

For ILCs, the cations are almost immobilized because they are much larger than anion and are linked to the adjacent cation by Van der Waals interactions. Therefore, the dominant charge carriers is thought to be anions.[13] As suggested by previous reports,[28,29] the total conductivity is given by the relation,

$$\sigma = nq\mu \approx n_{anion}q\mu_{anion} \quad (4)$$

Where n is the number of dissociated charge carriers per unit volume, q is the charge carried by them, and μ is the mobility of the carriers. Therefore, any change in the number of charge carriers and/or in the mobility will result in changing the total conductivity value. As mentioned above, with the increasing x, the layer spacing d of $C_{12}MIm(BF_4)_yI_x$ keeps increasing, resulting in the reduction of the number of ion-conductive layers per unit volume, namely, n_{anion}. On the other hand, μ_{anion} is expected to relate to the hydrogen bond between the anions and protons of imidazolium cations.[30] According to eqn (2), we may obtain that μ of BF_4^- is larger than that of I^-. Therefore, $\sigma_{\parallel}$and $\sigma_{\perp}$ of $C_{12}MImBF_4$ are larger than that of $C_{12}MImI$. According to eqn (3), with the increase of x, the ability of $[(BF_4)_yI_x]^-$ to form a three dimensional hydrogen bond with imidazolium cations increases, which would result in the decrease of the mobility of the anions. As a result, combining the changing of n_{anion} with x, the anisotropic ionic conductivity of $C_{12}MIm(BF_4)_yI_x$ decreases with the increasing content of $C_{12}MImI$.

3.2 Multi-component system

3.2.1 Mesogenic properties of $C_{12}MIm(BF_4)_{0.4}I_{0.45}(I_3)_{0.15}$. It is known that I^- can easily react with I_2 and form I_3^-. Herein, a certain content of I_2 is introduced to the binary system $C_{12}MIm(BF_4)_{0.4}I_{0.6}$ ($[C_{12}MImI] : [I_2] = 4 : 1$), and in the multi-component system I^-, BF_4^- as well as I_3^- co-exist. The effects of I_3^- on the mesophase temperature range of $C_{12}MIm(BF_4)_{0.4}I_{0.6}$ are shown in Fig. 7 and Table 2. It is found that a mesophase is also formed in multi-component system $C_{12}MIm(BF_4)_{0.4}I_{0.45}(I_3)_{0.15}$. Compared with binary system $C_{12}MIm(BF_4)_{0.4}I_{0.6}$, both the melting point and clearing point of $C_{12}MIm(BF_4)_{0.4}I_{0.45}(I_3)_{0.15}$ decrease, which results in a relatively lower mesophase temperature range. I_3^- can be seen as a coordination ion which is composed of a central atom (I) and two co-ordinate ions (I). According to eqn (1) the charge density of the co-ordinate ion I is also <1. Therefore, the ability of anions to form a three dimensional hydrogen bond will have the following relation,

$$[(BF_4)_{0.4}I_{0.45}(I_3)_{0.15}]^- < [(BF_4)_{0.4}I_{0.6}]^- \quad (5)$$

Thus, the mesophase stability of $C_{12}MIm(BF_4)_{0.4}I_{0.45}(I_3)_{0.15}$ decreases. As for the melting point, it may be associated with the interaction energy.[27,31] Due to the relative lower charge density of I in I_3^- and the larger radius of I_3^-, coulombic interactions between I_3^- and cations will be weakened compared with those between I^- and cations. Consequently, the melting point of $C_{12}MIm(BF_4)_{0.4}I_{0.45}(I_3)_{0.15}$ decreases. Additionally, since the

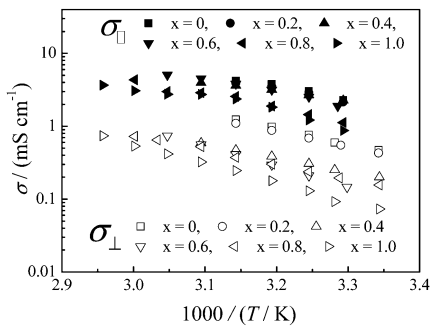

Fig. 6 Anisotropic ionic conductivities for $C_{12}MIm(BF_4)_yI_x$.

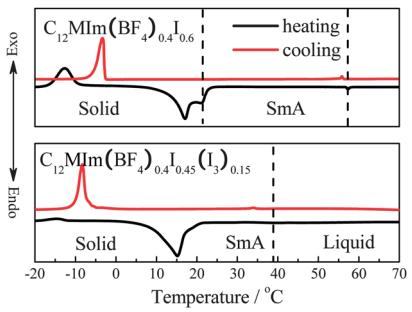

Fig. 7 DSC heating and cooling traces of $C_{12}MIm(BF_4)_{0.4}I_{0.6}$ and $C_{12}MIm(BF_4)_{0.4}I_{0.45}(I_3^-)_{0.15}$.

Table 2 A summary of the thermal analysis for $C_{12}MIm(BF_4)_{0.4}I_{0.6}$ and $C_{12}MIm(BF_4)_{0.4}I_{0.45}(I_3^-)_{0.15}$

	Heating		Cooling		
Ionic liquid crystals	T/(°C)	ΔH/(kJ mol^{-1})	T/(°C)	ΔH/(kJ mol^{-1})	Phase transition
$C_{12}MIm(BF_4)_{0.4}I_{0.6}$	57.32	0.30	55.87	−0.28	Lc–L
	21.26	2.03	−3.28	−14.51	S–Lc
	16.90	12.21	—	—	[a]S1–S
	−12.73	−11.91	—	—	[a]S2–S1
$C_{12}MIm(BF_4)_{0.4}I_{0.45}(I_3)_{0.15}$	38.70	0.19	34.08	−0.18	Lc–L
	15.16	27.68	−8.30	−14.01	S–Lc
	−14.73	−1.38	−28.58	−0.07	S1–S

[a] "S2–S1" and "S1–S" denote the phase transition from solid to solid.

cation in $C_{12}MIm(BF_4)_{0.4}I_{0.45}(I_3)_{0.15}$ is the same as that in $C_{12}MIm(BF_4)_{0.4}I_{0.6}$, the structure of $C_{12}MIm(BF_4)_{0.4}I_{0.45}(I_3)_{0.15}$ resembles that of $C_{12}MIm(BF_4)_{0.4}I_{0.6}$, that is, an interdigitated bilayer structure is formed in $C_{12}MIm(BF_4)_{0.4}I_{0.45}(I_3)_{0.15}$ (Fig. S7† and S8†).

3.2.2 Diffusion of iodide species in $C_{12}MIm(BF_4)_{0.4}I_{0.45}(I_3)_{0.15}$. As mentioned above, the existence of the smectic layer would benefit the ionic conductivity, because the SmA phase provides a two-dimensional conductive path in the interlayer regions and consequently facilitates the electric conductivity. Besides, it may also benefit the diffusion of iodide species. The diffusion of iodide species in ILC $C_{12}MIm(BF_4)_{0.4}I_{0.45}(I_3)_{0.15}$ was measured by the ultra-microelectrode technique.[32] An IL composed of $C_{12}MImBF_4$, 1-undecyl-3-methylimidazolium iodide ($C_{11}MImI$) and I_2 is used as the reference and the IL is denoted $[(C_{12}MImBF_4)_{0.4}(C_{11}MIm)_{0.6}I_{0.45}(I_3)_{0.15}]$. The molar ratio of $C_{12}MImBF_4$, $C_{11}MImI$ and I_3 in $[(C_{12}MImBF_4)_{0.4}(C_{11}MIm)_{0.6}I_{0.45}(I_3)_{0.15}]$ is the same as in $C_{12}MIm(BF_4)_{0.4}I_{0.45}(I_3)_{0.15}$, and no mesophase is observed in $[(C_{12}MImBF_4)_{0.4}(C_{11}MIm)_{0.6}I_{0.45}(I_3)_{0.15}]$. Fig. 8 shows the steady-state voltammograms of $C_{12}MIm(BF_4)_{0.4}I_{0.45}(I_3)_{0.15}$ and $[(C_{12}MImBF_4)_{0.4}(C_{11}MIm)_{0.6}I_{0.45}(I_3)_{0.15}]$ at 300 K. The diffusion flux of I_3^- can be obtained from the following equation,[32]

$$D_{I_3^-}c_{I_3^-} = \frac{I_s}{4nFr} \quad (6)$$

Where I_s is steady-state current of I_3^-, $D_{I_3^-}$ is the apparent diffusion coefficient of I_3^-, $c_{I_3^-}$ is the bulk concentration of I_3^-, n is the electron transfer number per molecule, F is the Faraday constant, and r is the radius of ultra-microelectrode.

From Fig. 8, it can be seen the I_s of I_3^- in ILC $C_{12}MIm(BF_4)_{0.4}I_{0.45}(I_3)_{0.15}$ is higher than that in IL $[(C_{12}MImBF_4)_{0.4}(C_{11}MIm)_{0.6}I_{0.45}(I_3)_{0.15}]$, indicating that the diffusion of I_3^- in $C_{12}MIm(BF_4)_{0.4}I_{0.45}(I_3)_{0.15}$ is faster than that in $[(C_{12}MImBF_4)_{0.4}(C_{11}MIm)_{0.6}I_{0.45}(I_3)_{0.15}]$ according to eqn (6). However, the viscosity of ILC $C_{12}MIm(BF_4)_{0.4}I_{0.45}(I_3)_{0.15}$ is larger than that of IL $[(C_{12}MImBF_4)_{0.4}(C_{11}MIm)_{0.6}I_{0.45}(I_3)_{0.15}]$, which means the physical diffusion in $C_{12}MIm(BF_4)_{0.4}I_{0.45}(I_3)_{0.15}$ is lower than that in $[(C_{12}MImBF_4)_{0.4}(C_{11}MIm)_{0.6}I_{0.45}(I_3)_{0.15}]$. This would lead to an idea that the exchange reaction based diffusion in $C_{12}MIm(BF_4)_{0.4}I_{0.45}(I_3)_{0.15}$ is higher than that in $[(C_{12}MImBF_4)_{0.4}(C_{11}MIm)_{0.6}I_{0.45}(I_3)_{0.15}]$. Because of the existence of the smectic layer in $C_{12}MIm(BF_4)_{0.4}I_{0.45}(I_3)_{0.15}$, the iodide species are located between the interdigitated layers, which increases the collision frequency of iodide species and consequently the diffusion based on the exchange reaction.[33]

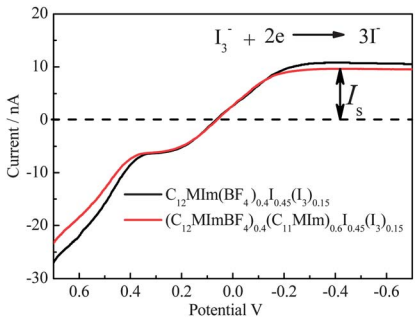

Fig. 8 Steady-state voltammograms of ILC $C_{12}MIm(BF_4)_{0.4}I_{0.45}(I_3)_{0.15}$ and IL $[(C_{12}MImBF_4)_{0.4}(C_{11}MIm)_{0.6}I_{0.45}(I_3)_{0.15}]$ at 300 K.

As we know, I^-/I_3^- are frequently used as charge carriers in the electrolyte used in dye-sensitized solar cells (DSCs) as discovered by Grätzel,[34] and the diffusion of iodide species plays a crucial role on the photovoltaic performance of DSCs. Thus, ILCs may be used to replace ILs as the electrolyte for DSCs due to their contribution to the exchange reaction based diffusion (Fig. S9†).

Conclusions

In summary, a series of binary systems based ionic liquid crystals (ILCs) $C_{12}MIm(BF_4)_yI_x$ ($x + y = 1$) are prepared by mixing the ILCs 1-dodecyl-3-methylimidazolium tetrafluoroborate ($C_{12}MImBF_4$) and 1-dodecyl-3-methylimidazolium iodide ($C_{12}MImI$). The effect of the molar proportion of $C_{12}MImBF_4$ and $C_{12}MImI$ on the mesogenic properties of $C_{12}MIm(BF_4)_yI_x$, including mesophase temperature range, layer spacings d as well as anisotropic ionic conductivity are systematically investigated. It is found that a SmA phase with interdigitated layers is formed in the $C_{12}MIm(BF_4)_yI_x$ series the same as in pure $C_{12}MImBF_4$ and $C_{12}MImI$. With the increasing content of $C_{12}MImI$ in $C_{12}MIm(BF_4)_yI_x$, the ability of $[(BF_4)_yI_x]^-$ to form a three dimensional hydrogen bond with cations increases, which results in the increase of the mesophase temperature range and layer spacing d as well as the decrease of the anisotropic ionic conductivity of $C_{12}MIm(BF_4)_yI_x$, including parallel ($\sigma_{\parallel}$) and perpendicular ($\sigma_{\perp}$) to the smectic layer. It is suggested that the binary systems $C_{12}MIm(BF_4)_yI_x$ combine the advantages of pure

$C_{12}MImBF_4$ and $C_{12}MImI$, and show a relatively larger mesophase temperature range than pure $C_{12}MImBF_4$ and higher anisotropic ionic conductivity than $C_{12}MImI$. Additionally, the multi-component system based ILC $C_{12}MIm(BF_4)_{0.4}I_{0.45}(I_3)_{0.15}$ is prepared by introducing iodine to binary system $C_{12}MIm(BF_4)_{0.4}I_{0.6}$. A SmA mesophase is also observed in $C_{12}MIm(BF_4)_{0.4}I_{0.45}(I_3)_{0.15}$, though some differences from $C_{12}MIm(BF_4)_{0.4}I_{0.6}$ in the mesophase temperature range are observed. Our results demonstrate that we can regulate the mesogenic properties of ILCs as we need by preparing binary or even multi-component systems. Furthermore, the smectic layer in $C_{12}MIm(BF_4)_{0.4}I_{0.45}(I_3)_{0.15}$ would benefit the diffusion coefficient of iodide species due to its contribution to the exchange reaction based diffusion, which exhibits potential applications in dye-sensitized solar cells.

Acknowledgements

This work was financially supported by the National Basic Research Program of China under Grant No. 2011CBA00700, the National High Technology Research and Development Program of China under Grant No. 2009AA050603, National High Technology Research and Development Program of China under Grant No. 2011AA050510, Funds of the Chinese Academy of Sciences for Key Topics in Innovation Engineering under Grant No. KGCX2-YW-326.

Notes and references

1 S. H. Fang, L. Yang, C. Wei, C. Jiang, K. Tachibana and K. Kamijima, *Electrochim. Acta*, 2009, **54**, 1752–1756.
2 J. Dupont, R. F. de Souza and P. A. Z. Suarez, *Chem. Rev.*, 2002, **102**, 3667–3691.
3 T. Welton, *Chem. Rev.*, 1999, **99**, 2071–2083.
4 M. Trilla, R. Pleixats, T. Parella, C. Blanc, P. Dieudonne, Y. Guari and M. W. C. Man, *Langmuir*, 2008, **24**, 259–265.
5 M. Yoshio, T. Kagata, K. Hoshino, T. Mukai, H. Ohno and T. Kato, *J. Am. Chem. Soc.*, 2006, **128**, 5570–5577.
6 N. Yamanaka, R. Kawano, W. Kubo, N. Masaki, T. Kitamura, Y. Wada, M. Watanabe and S. Yanagida, *J. Phys. Chem. B*, 2007, **111**, 4763–4769.
7 C. K. Lee, H. W. Huang and I. J. B. Lin, *Chem. Commun.*, 2000, 1911–1912.
8 R. G. Weiss, *Tetrahedron*, 1988, **44**, 3413–3475.
9 C. F. J. Faul and M. Antonietti, *Adv. Mater.*, 2003, **15**, 673–683.
10 C. M. Gordon, J. D. Holbrey, A. R. Kennedy and K. R. Seddon, *J. Mater. Chem.*, 1998, **8**, 2627–2636.
11 J. D. Holbrey and K. R. Seddon, *J. Chem. Soc., Dalton Trans.*, 1999, 2133–2139.
12 W. Dobbs, L. Douce, L. Allouche, A. Louati, F. Malbosc and R. Welter, *New J. Chem.*, 2006, **30**, 528–532.
13 F. Xu, K. Matsumoto and R. Hagiwara, *Chem.–Eur. J.*, 2010, **16**, 12970–12976.
14 C. J. Bowlas, D. W. Bruce and K. R. Seddon, *Chem. Commun.*, 1996, 1625–1626.
15 A. Getsis and A. V. Mudring, *Cryst. Res. Technol.*, 2008, **43**, 1187–1196.
16 K. Binnemans, *Chem. Rev.*, 2005, **105**, 4148–4204.
17 A. E. Bradley, C. Hardacre, J. D. Holbrey, S. Johnston, S. E. J. McMath and M. Nieuwenhuyzen, *Chem. Mater.*, 2002, **14**, 629–635.
18 R. Hagiwara, K. Matsumoto, Y. Nakamori, T. Tsuda, Y. Ito, H. Matsumoto and K. Momota, *J. Electrochem. Soc.*, 2003, **150**, D195–D199.
19 Y. J. Huang, Y. H. Cong, J. J. Li, D. L. Wang, J. T. Zhang, L. Xu, W. L. Li, L. B. Li, G. Q. Pan and C. L. Yang, *Chem. Commun.*, 2009, 7560–7562.
20 M. Yoshio, T. Mukai, H. Ohno and T. Kato, *J. Am. Chem. Soc.*, 2004, **126**, 994–995.
21 M. Yoshio, T. Kato, T. Mukai, M. Yoshizawa and H. Ohno, *Mol. Cryst. Liq. Cryst.*, 2004, **413**, 2235–2244.
22 J. Y. Z. Chiou, J. N. Chen, J. S. Lei and I. J. B. Lin, *J. Mater. Chem.*, 2006, **16**, 2972–2977.
23 P. B. Hitchcock, K. R. Seddon and T. Welton, *J. Chem. Soc., Dalton Trans.*, 1993, 2639–2643.
24 N. Yamanaka, R. Kawano, W. Kubo, T. Kitamura, Y. Wada, M. Watanabe and S. Yanagida, *Chem. Commun.*, 2005, 740–742.
25 K. Goossens, P. Nockemann, K. Driesen, B. Goderis, C. Gorller-Walrand, K. Van Hecke, L. Van Meervelt, E. Pouzet, K. Binnemans and T. Cardinaels, *Chem. Mater.*, 2008, **20**, 157–168.
26 J. De Roche, C. M. Gordon, C. T. Imrie, M. D. Ingram, A. R. Kennedy, F. Lo Celso and A. Triolo, *Chem. Mater.*, 2003, **15**, 3089–3097.
27 W. M. Reichert, J. D. Holbrey, R. P. Swatloski, K. E. Gutowski, A. E. Visser, M. Nieuwenhuyzen, K. R. Seddon and R. D. Rogers, *Cryst. Growth Des.*, 2007, **7**, 1106–1114.
28 M. Wang, X. Yin, X. R. Mao, X. W. Zhou, Z. Z. Yang, X. P. Li and Y. Lin, *J. Photochem. Photobiol., A*, 2008, **194**, 20–26.
29 B. Bhattacharya, J. Y. Lee, J. Geng, H. T. Jung and J. K. Park, *Langmuir*, 2009, **25**, 3276–3281.
30 P. A. Hunt, *J. Phys. Chem. B*, 2007, **111**, 4844–4853.
31 D. M. Li, M. Y. Wang, J. F. Wu, Q. X. Zhang, Y. H. Luo, Z. X. Yu, Q. B. Meng and Z. J. Wu, *Langmuir*, 2009, **25**, 4808–4814.
32 P. Wang, S. M. Zakeeruddin, J. E. Moser, M. K. Nazeeruddin, T. Sekiguchi and M. Grätzel, *Nat. Mater.*, 2003, **2**, 402–407.
33 R. Kawano and M. Watanabe, *Chem. Commun.*, 2005, 2107–2109.
34 B. Oregan and M. Grätzel, *Nature*, 1991, **353**, 737–740.